In Situ and Self-Restorable Injection-Locking Monitor by Integrated Photodiode for FPLD WDM Transmitter

Gong-Ru Lin, *Senior Member, IEEE,* Yu-Sheng Liao, and Hao-Chung Kuo

***Abstract*—A novel *in situ* self-restoration scheme to track real time the injection locking of a Fabry-Perot laser diode (FPLD) is demonstrated by a built-in integrated monitor photodiode (MPD). The variation in the received photocurrent of the integrated MPD was calculated by a microcontroller unit integrated with an analog-to-digital converter, which is employed to dynamically control the temperature of the FPLD via a thermal-electrical controller for wavelength stabilization. Such a scheme can be effectively implemented with a minimum amount of redundant network resources to achieve self-restoration within 50 s with Q factor >8.2 and side-mode suppression ratio >35 dB at 2.5 Gbit/s. The feasibility of the proposed self-restorable locker is suitable for most wavelength-locking FPLDs within high-speed wavelength-division multiplexing networks.**

***Index Terms*—Auto restoration, Fabry-Perot laser diode, injection locking, monitored photodiode, real time.**

I. Introduction

The application of wavelength-division multiplexing (WDM) in local access networks is a promising approach to meet the demand of increasing bandwidths required in the near future. However, the relatively high cost of the transmitters with specified wavelengths has hindered market acceptance. In this context, the injection-locked Fabry-Perot laser diode (FPLD) has received substantial attention [1] as it can produce a single longitudinal mode with a high side-mode suppression ratio (SMSR) for potential applications in the WDM optical communications. In principle, the injection-locking lasers strictly rely on external seeding or self-feedback injecting a continuous-wave (CW) laser to achieve single-mode pulsed generation. Many versatile injection-locking techniques, such as the clock frequency division [2], the 10 Gb/s WDM passive optical network (PON) [3], the parallel transmission and wavelength routing network (Para-Wave NET) [4], and the all-optical nonreturn-to-zero to pseudo-return-to-zero (PRZ) format transformation [5], have been demonstrated. All these applications require precisely controlled injection-locked FPLD, but the maintenance as regards its stability and reliability usually requires complicated modules. Therefore, fault management is one of the crucial aspects in network management to enhance the network reliability. Of late, many efforts have been focused on the fault-monitoring methods [6] and the self-restorable networks [7] to achieve network protection.

In this paper, a novel *in situ* injection-locking monitor for real-time and self-restorable tracking the FPLD-based WDM-PON transmitter is shown. Without employing high-speed electronics and instruments, the proposed *in situ* monitoring and self-restorable architecture uses the integrated monitor photodiode (MPD), which is usually employed to monitor the optical power illuminated by the FPLD. An embedded 8 bit commercial microcontroller-unit (MCU) is used to achieve the real-time and self-restorable control, which can be easily added into injection-locking systems for getting higher reliability. It is cost effectively implemented with a minimum amount of redundant network resources and the MPD-based autopower-control (APC) function, which can simultaneously be integrated in the proposed system to optimize the optoelectronic performance of the FPLD.

II. Experimental Setup

Fig. 1 schematically illustrates an *in situ* and self-restorable architecture for injection-locked FPLD WDM transmitter. A fiberoptic WDM transmitter with a standard package of Transistor Outline (TO)-56 can is shown in the inset of Fig. 1. The typical front-facet and back-facet reflectivity of their FPLD used in the system is 30% and 90%, respectively. In other words, the front facet of the FPLD is uncoated and the back facet of the FPLD is high-reflection (HR) coated. It is necessary to keep the reflectivity of FPLD at a certain value to make its mode-extinction ratio sufficiently large for distinguishing the lock-in from loose-lock condition. The self-restoration unit cannot work for an FPLD without sufficiently large discrimination between longitudinal modes. The output power of the FPLD chip is 6 mW at 30 mA, and its coupling efficiency to a single-mode fiber is about 15%. The electrical frequency response of the directly modulated FPLD was mea-

Manuscript received February 1, 2010; revised April 17, 2010; accepted April 26, 2010. Date of current version December 30, 2010. This work was supported in part by the National Science Council, under Grants NSC96-2221-E-002-099 and NSC-98-2221-E-002-023-MY3.

G.-R. Lin is with the Graduate Institute of Photonics and Optoelectronics, and Department of Electrical Engineering, National Taiwan University, Taipei 106, Taiwan (e-mail: grlin@ntu.edu.tw).

Y.-S. Liao and H.-C. Kuo are with the Department of Photonics, and Institute of Electro-Optical Engineering, National Chiao Tung University, Hsinchu 300, Taiwan.

Color versions of one or more of the figures in this paper are available online at http://ieeexplore.ieee.org.

Digital Object Identifier 10.1109/JQE.2010.2049643

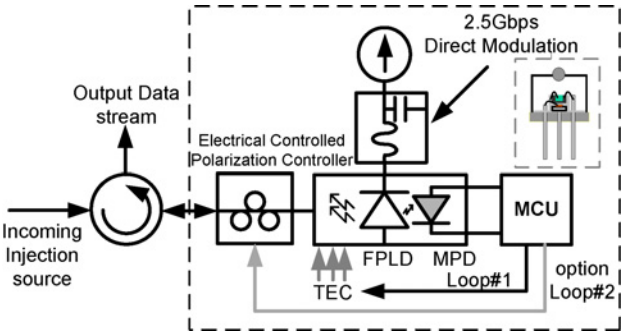

Fig. 1. Self-restorable system for injection-locked FPLD with monitor photodiode. The MCU detects the MPD photocurrent and controls the TEC and the polarization controller.

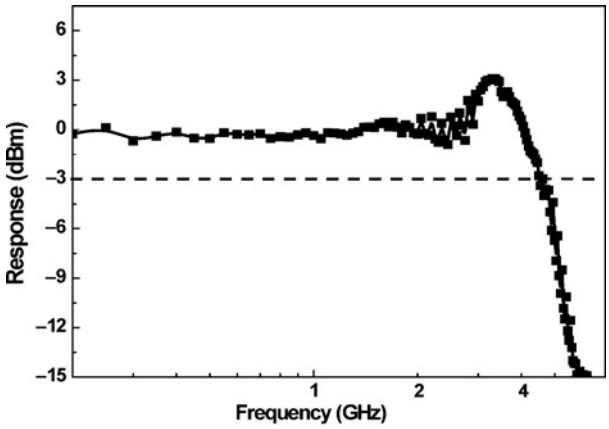

Fig. 2. Frequency response of the directly modulated FPLD with 3 dB bandwidth of 4.2 GHz.

sured by a lightwave component analyzer (HP, $f_{\mathrm{mod}} > 20$ GHz, 8703A), as shown in Fig. 2, and the FPLD exhibits the 3 dB bandwidth of 4.2 GHz. The MPD was placed on the HR coated side of the FPLD and the photocurrent is fed back to the MCU-based auto-restorable controller. A tunable laser (TL, ANDO 4321D) with a wavelength resolution of 0.001 nm is employed as the master laser for injection locking the FPLD.

An MCU (ATMEL MEGA88V)-integrated analog-to-digital converter (ADC) recurrently measures the photocurrent of the MPD every 0.1 ms and dynamically controls the temperature of the thermal-electronic controller (TEC). The FPLD exhibits a threshold current of 8.5 mA, a longitudinal mode spacing of 1.15 nm, and a peak wavelength of 1533.5 nm. Herein, the DC bias current of the FPLD is set as 30 mA and the amplitude of the RF signal is set to reach the optical extinction ratio of 10 dB by directly modulating the FPLD. The FPLD temperature is controlled at 30 °C with <0.1 °C fluctuation to prevent the wavelength drift of each longitudinal mode. The temperature-dependent wavelength shifting slope is 0.06 nm °C. Another function to achieve the self-restoration of the preferred polarization for the FPLD is based on feedback controlling an electronically tunable polarization controller added prior to the FPLD to be injection-locked as shown in the Loop#2 in Fig. 1. The proposed scheme cannot eliminate the polarization sensitive problem accompanied with the injection-locked FPLD, however, the MCU of self-restorable injection

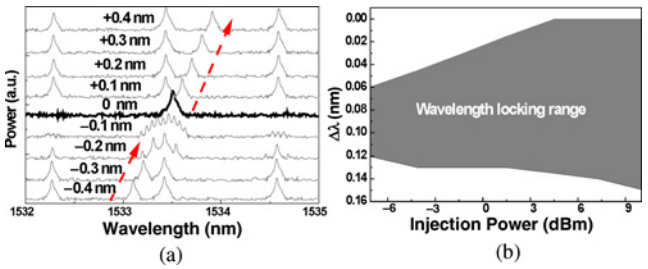

Fig. 3. (a) Spectrum evolution of FPLD by detuning per 0.1 nm wavelength. (b) Wavelength locking range of a side mode in the slave FPLD as a function of injection-locked power.

locker can concurrently deal both the deviation of FPLD wavelength and the mismatched polarization of the incoming light.

III. Results and Discussion

A. Modeling and Experimental Results of the Injection-Locking Output Power Variation of FPLD

Fig. 3(a) illustrates the injection-locking wavelength evolution by detuning the injection wavelength, in which the black line shows the exact injection locking condition. As a result, the wavelength-locking range of the slave FPLD measured by adopting the modified delayed self-homodyne scheme [8], which is used to determine the stability of injection locking by monitoring the reduction of the injection-locked FPLD mode linewidth, is shown in Fig. 3(b). The detuning wavelength is defined as the wavelength shift of the master TL with respect to one longitudinal mode of the slave FPLD by obtaining SMSR >35 dB. Fig. 3(a) shows that <2 °C accuracy must be satisfied when using injection-locked FPLD. Fig. 3(b) shows that <0.09 nm wavelength accuracy must be satisfied at > -3 dBm injection, and the temperature of FPLD should be controlled within 1.5 °C. However, the inevitable aging of the FPLD is an important issue in practical telecommunication systems.

By adjusting the FPLD driving currents at 25, 30, 35 mA and detuning its wavelength to realize the injection locking, the results shown in Fig. 4(a) indicate a notable peak photocurrent at exactly injection locking, which leads to the maximum output power of FPLD. Fig. 4(b) illustrates the behavior of the MPD at injection power of +3, 0, −3, −6, and −9 dBm versus detuning wavelength. A minimum injection power of −9 dBm for all longitudinal modes is required to initiate the wavelength locking. The red-shifted detuning wavelength of the master laser with respect to the free-running longitudinal mode of slave laser was also observed by Bouchoule *et al.* [9]. The carrier density of FPLD can be severely depleted at a larger gain region to cause the redshift in locking the wavelength range. In addition, a relatively weak signal with considerable noise generated by multi-longitudinal-mode beating effect has also been found as the injection wavelength is detuned away from the slave FPLDs longitudinal mode by 0.14 nm. The largest illuminated power occurs at the center wavelength of a longitudinal mode exactly located at the injection wavelength to achieve exact injection locking. By detuning injection wavelength, the amplified photocurrent phenomenon at an

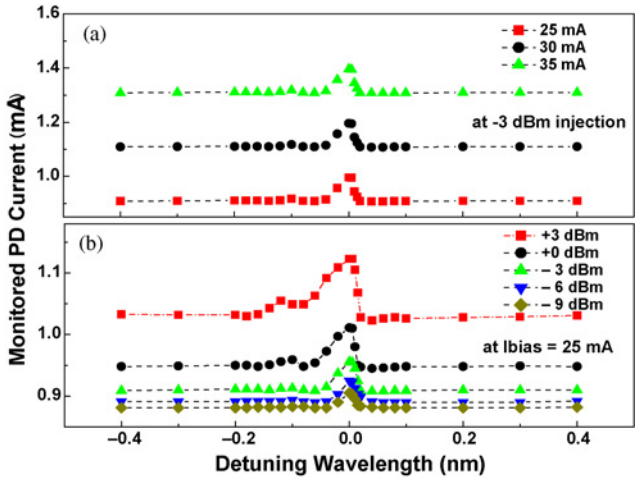

Fig. 4. (a) Photocurrent of MPD at the FPLD driving currents of 25, 30, and 35 mA as detuning wavelength. (b) Photocurrent of MPD at the injection power of +3, 0, −3, −6, and −9 dBm as detuning wavelength.

exact injection-locking condition will be reduced by shifting the injection wavelength from the central wavelength of this longitudinal mode. The photon density in the FPLD gradually decays with detuning injection wavelength. Concurrently, the carrier density in the FPLD is persistently depleted under the external injection, even though the injection wavelength deviates from the central wavelength.

Such a fringe-like photocurrent enhancement effect is mainly caused by the Fabry-Perot etalon. The mode extinction ratio of the FPLD is reduced by attenuating the front or back reflectivity, and thus the sharpness of the transmission function. This clearly elucidates the rapidly decayed gain around central mode wavelength. By injecting each longitudinal mode at −9 dBm, Fig. 4(a) illustrates a similarly monitored photodetector (PD) photocurrent feature, where the FP etalon effect dominates the monitored PD photocurrent response. As the FPLD is externally seeded by a single-mode laser source, the carriers in the FPLD were depleted under the external seeding. The power gain of the FPLD lasing mode spectrum by involving the Fabry-Perot etalon effect is described as

$$G_T(\lambda) = G_0 \frac{(1-R_1)R_2}{\left(1-\sqrt{R_1}\sqrt{R_2}e^{2g(\lambda)d}\right)^2} \frac{e^{4g(\lambda)d}}{1+\dfrac{4\sqrt{R_1}\sqrt{R_2}e^{2g(\lambda)d}}{\left(1-\sqrt{R_1}\sqrt{R_2}e^{2g(\lambda)d}\right)^2}\sin^2\left(\lambda\pi/\Delta\lambda_m\right)} \tag{1}$$

where $g(l)$ is the differential gain as a function of wavelength and d the cavity length. R_1 and R_2 are the reflectivity of the front and rare facets, respectively. The phase difference d in the standard Fabry-Perot etalon equation can be replaced by the free spectrum range $\mathrm{Dl_m}$. In particular, the mechanism responsible for gain and output power variations of the FPLD is also discussed, which facilitate the mode discrimination by distinct PD current change between the locking and the unlocking conditions. Assuming one longitudinal mode under external injection-locking condition, the gain of FPLD, $G(N, S)$, can be described as [10]

$$\begin{aligned} G\left(N_{\mathrm{inj}}, S_{\mathrm{inj}}\right) &= G_N\left(N_{\mathrm{inj}} - N_0\right)\left(1 - k_s S_{\mathrm{inj}}\right) \\ &= G_N\left(N_{th} - N_0\right) + \Delta G\frac{1}{\tau_p} + D_G + G_N\Delta N - G_s\Delta S \\ &= \frac{1}{\tau_p} - \frac{R_{\mathrm{sp}}}{S_{\mathrm{LD}}} - \sqrt{\frac{4\alpha^2k_c^2}{\left(1+\alpha^2\right)}}\sqrt{\frac{S_{\mathrm{inj}}}{S_{\mathrm{LD}}}} \end{aligned} \tag{2}$$

where N_{inj} is the carrier number of the FPLD under external injection locking, S_{inj} the externally injected photon number, N_0 the transparent carrier number, N_{th} the threshold carrier number, DG the gain change, t_p the photon lifetime, D_G the normalized gain difference, G_N and G_s are the differential gain coefficients for DN and DS denoting the variations of carrier and photon numbers, respectively. R_{sp} denotes the spontaneous emission rate, and S_{LD} the total photon number at the injection-locked mode, a the linewidth broadening factor, and k_c the coupling coefficient of the FPLD for external injection. The derivation indicates that the gain of FPLD is reduced under the external injection-locking condition. On the other hand, the variation on threshold current (I_{th}) of FPLD from the change of carrier number under external injection-locking condition is given in [5], [10], [11]

$$\begin{aligned} N_{\mathrm{th,inj}} &= \frac{G\left(N_{\mathrm{inj}}, S_{\mathrm{inj}}\right)}{G_N} + N_0 \\ &= \frac{1}{G_N}\left[\frac{1}{\tau_p} - \frac{R_{\mathrm{sp}}}{S_{\mathrm{LD}}} - \sqrt{\frac{4\alpha^2k_c^2}{\left(1+\alpha^2\right)}}\sqrt{\frac{S_{\mathrm{inj}}}{S_{\mathrm{LD}}}}\right] + N_0 \end{aligned} \tag{3}$$

$$\begin{aligned} I_{\mathrm{th,inj}} &= \frac{q}{\eta_i\tau_c}N_{\mathrm{th,inj}} = \frac{q}{\eta_i\tau_c}\left[\frac{1}{G_N}\left(\frac{1}{\tau_p} - \frac{R_{\mathrm{sp}}}{S_{\mathrm{LD}}} - \sqrt{\frac{4\alpha^2k_c^2}{\left(1+\alpha^2\right)}}\sqrt{\frac{S_{\mathrm{inj}}}{S_{\mathrm{LD}}}}\right) + N_0\right] \\ &= \frac{q}{\eta_i\tau_c}\left(\frac{1}{G_N\tau_p} + N_0\right) - \frac{q}{\eta_i\tau_c G_N}\left(\frac{R_{\mathrm{sp}}}{S_{\mathrm{LD}}} + \sqrt{\frac{4\alpha^2k_c^2}{\left(1+\alpha^2\right)}}\sqrt{\frac{S_{\mathrm{inj}}}{S_{\mathrm{LD}}}}\right) \end{aligned} \tag{4}$$

where q denotes the electron charge, h_i the internal quantum efficiency, and t_c the carrier lifetime. The threshold current of FPLD is also decreased due to the external injection. The output power of the FPLD can thus be written as

$$\begin{aligned} P_{\mathrm{out,inj}} &= \eta_d\frac{h\nu}{q}\left(I - I_{\mathrm{th,inj}}\right) \\ &= \eta_d\frac{h\nu}{q}\left\{I - \frac{q}{\eta_i\tau_c}\left(\frac{1}{G_N\tau_p} + N_0\right) + \frac{q}{\eta_i\tau_c G_N}\left(\frac{R_{\mathrm{sp}}}{S_{\mathrm{LD}}} + \sqrt{\frac{4\alpha^2k_c^2}{\left(1+\alpha^2\right)}}\sqrt{\frac{S_{\mathrm{inj}}}{S_{\mathrm{LD}}}}\right)\right\} \\ &= \eta_d\frac{h\nu}{q}\left(I - I_{\mathrm{th},0}\right) + \eta_d\frac{h\nu}{q}\Delta I_{\mathrm{inj}} \equiv P_{\mathrm{out},0} + \Delta P \end{aligned} \tag{5}$$

where h_d is indeed the differential quantum efficiency, hn the energy per photon, and I_{th} the threshold current. Both the gain and the threshold current of the FPLD are decreased under external injection-locking condition. The reduced gain fails to amplify the injected signal, whereas the improvement on the output power of the FPLD is completely due to threshold current reduction.

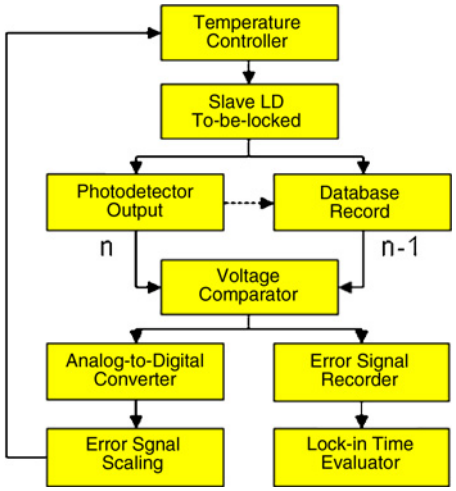

Fig. 5. Conceptual flow chart for designing the PD-MCU link based self-restoration unit.

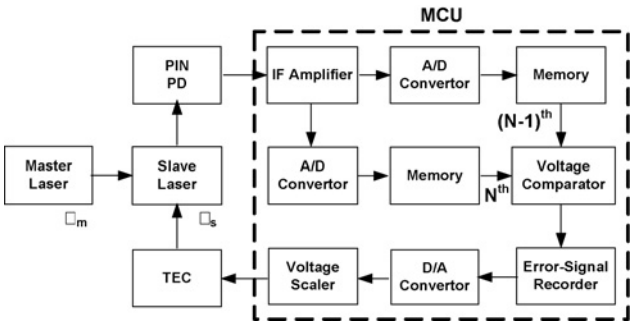

Fig. 6. Circuit block for building a PD-MCU link based self-restoration unit.

B. Concept and Circuit Design of MPD-MCU Based Auto-Restorable FPLD Transmitter

The concept of the *in situ* PD and MCU-based self-restoration system is derived from the fault-finding and restoration functions comprehensively used in optical time-domain reflectometry (OTDR) system for maintaining the cabling system's functionality. The principle of self-restoration in a conventional OTDR is based on to the transmission-line theory, which detects impedance or reflectance change of the optical pulse when reflecting from the break-up node along a fiber cable. Such an impedance change is reflected back and the OTDR measures the time taken for the reflection to return and converts this into distance along the fiber cable. An MCU is usually employed for the time-distance conversion in the OTDR; however, there is no requirement on the additional feedback circuitry for further control. Based on this concept, the flow chart for designing such a PD-MCU link in our system is plotted in Fig. 5. In the injection-locked laser diode system, the slave laser output power is a function of independent variables, such as the master laser injecting wavelength and the specific longitudinal-mode wavelength of slave laser (which is tunable with the changing temperature). Thus, the PD-MCU system is constructed in response to the input signal from the injection-locked slave laser by producing an error signal feedback to control the temperature of the slave laser diode.

In more detail, the signal input to the MCU is obtained by optoelectronically converting the injection-locked laser diode output power via the photodetector, and the converted voltage signal is used as the input to a MCU with a program for an automated diagnosis of injection-locking condition. The MCU compares the input signal amplitude with the recorded amplitude in its memory, and then responds by producing an error signal to feedback control the operating temperature of the laser diode. As a result, the wavelength of the gain spectrum as well as the longitudinal modes in the laser diode can be shifted by the feedback temperature control, thus providing an improved injection locking with the incoming master laser signal at a deviated wavelength. After a relatively short duration, the voltage comparator in MCU delivers zero-error voltage when the converted output signal amplitude from the injection-locked laser diode no longer changes, as the initiation of feedback control by the PD-MCU based self-restoration system has eventually forced the longitudinal wavelength laser diode coincident with the incoming master wavelength. The digital/discrete circuit blocks are used to process these signals in the MCU, which is converted back to analog/continuous signals for temperature control afterward. This results in the self-restoration of the wavelength of the injection-locked slave laser diode. Such a PD-MCU link essentially enhances the real-time wavelength restoration and error-noise suppression abilities through the digitized voltage comparator and feedback controller. The circuit block for building such a PD-MCU link is illustrated in Fig. 6.

Indeed, such injection-locked laser diodes still exhibit a benefit on narrow linewidth, long transmission distance, and especially the enhanced modulation bandwidth when comparing with other kinds of injection-locked sources. Nevertheless, both of wavelength matching and polarization matching are the important issues of the injection-locked FPLD for its application on communication network systems. In particular, the polarization control is the unique and inherent problem when utilizing the injection locking technique to control the laser diode wavelength. If the polarization state of the external injection is vertical to that of the FPLD, the eye diagram is worse than the injection-locked case and the bit-error rate (BER) is slightly degraded with a power penalty of 3 dB. However, the FPLD can still be used for data transmission since which is operated at free-running mode as compared to the injection-locked mode in this case. If the wavelength of the incoming light is also deviated without self-restoration, the BER performance of the FPLD under polarization mismatched condition is almost identical to that of the FPLD works at free-running condition. That is, the polarization degree directly affects the injection efficiency, which is a little bit different from the wavelength detuning effect. The requested power of optical injection into the FPLD could be greatly increased due to the deviation of the injected polarization from the preferred state of the FPLD. In our self-restorable design, the concept to achieve the self-restoration of the preferred polarization for the FPLD is based on feedback controlling an electronically tunable polarization controller added prior to the FPLD to be injection-locked. The MPD current of the FPLD is monitored

during operation for feedback controlling the polarization controller to obtain the maximum output power from the injection-locked FPLD. After comparing the monitored MPD current with previous value, the MCU sends a controlling signal to detune incoming polarization via a polarization controller (see Loop#2 in Fig. 1). With the same feedback control loop, the two important issues of wavelength locking and polarization matching can be concurrently implemented for the practical self-restorable injection locker. Based on the proposed self-restorable injection locker for the injection-locked FPLD, both the wavelength deviation and polarization mismatch between the FPLD and the incoming light can be effectively feedback controlled to optimize the injection-locking performance, which makes the self-restorable injection-locked FPLD more practical for data transmission in network system.

C. Auto-Restorable Injection-Locking Performances of the MPD-MCU Based System

Later on, the analysis of auto-restorable architecture is performed to characterize the auto-injection-locking performance of a directly modulated FPLD in a 2.5 Gbit/s WDM fiberoptic network. To achieve auto-restoration, the MCU plays an important role in detecting and calculating the MPD photocurrent, and decides whether to increase or decrease the slave-FPLD temperature by feedback TEC. The TO-can of FPLD is clamped to the aluminum block to ensure the TO-can at the ambient temperature. While a sudden unlocking event occurs with a monitored photocurrent located in gradient MPD current region, the MCU can correctly determine the detuning direction by comparing the derivative photocurrent. However, if the sudden unlocking wavelength is located in the flattened gain region, the auto-restoration will directly control the slave FPLD wavelength toward the next longitudinal mode to be injection locked. The positive-wavelength searching further benefits from the early wavelength peak detection in most conditions. In experiment, the injection wavelength is blue-shifted by 0.8 nm and the injection power is set at −9 dBm to simulate the practical condition at the unlocking state. The 0.8 nm shift is indeed a relatively worse case for demonstrating the self-restoration system with a positive wavelength searching function (increase temperature). Concurrently, the mode spacing and the temperature drift rate were preset in the MCU.

For each slave FPLD under self-restoration operation, all the parameters are not necessarily calibrated as the MCU can automatically lock-in the desired mode by detecting the optimized point. The MPD current remains almost constant when the self-restoration is completed by tuning the FPLD longitudinal mode coincidently with the injecting wavelength, as shown in Fig. 7(a). By detuning the injecting source at different wavelengths, the injection-locked output spectra can be obtained and shown in Fig. 7(b). As tuning over the specific longitudinal mode, the photocurrent is rapidly decayed due to the Fabry-Perot etalon enhanced gain competition effect. Overheating instead of the gradient variation searching method was used in our system to enhance the locking time, while the MCU program performs more like a binary searching function to reach the mode restoration within three damping cycles. In general, such a self-restoration can be achieved within 10 s

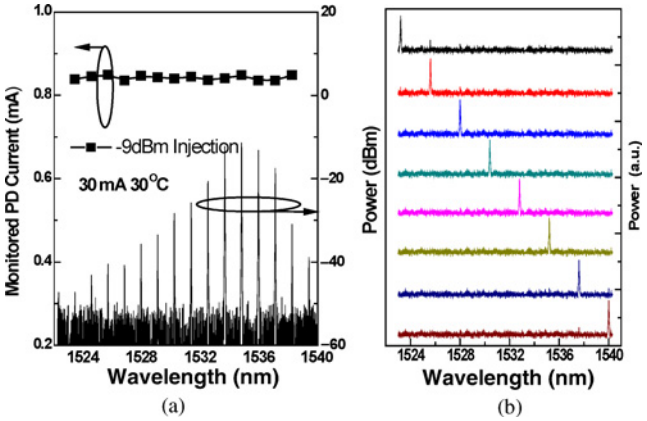

Fig. 7. (a) Monitored PD current (upper, square-dotted curve) and the free-running FPLD spectrum (lower, block lines). (b) Spectra of the FPLD transmitter injection locked at different longitudinal modes (color lines at right part).

(limited by the TEC tuning speed). Even with such a bad case for a slave FPLD with an external TEC module, the injection locking can still be obtained within 50 s and the correct temperature can be recovered with 0.1 °C resolution, as shown in Fig. 6. This figure is obtained with an injecting power of −3 dBm with a monitored PD current of about 1 mA at stabilized injection-locking condition. In the system proposed here, the lowest injection power can be −9.0 dBm, which is limited by the background noise level and by the resolution of the ADC circuit in MCU.

On the other hand, the injection power cannot be increased too high as it may damage the coupling end-face of the FPLD transmitter. Moreover, the additional reflectance from the FPLD coupling end-face is up to 1.5% (assume the coupling efficiency of the TO-can ball lens is 15%, and the front-face reflectivity of the FPLD is 70%). The FPLD output power could saturate at higher injection levels, whereas the reflection from coupling end does not saturate with increasing injection power. As a result, the FPLD transmitted data stream will be carried by a DC offset due to the additional coupling end-face reflection. In this case, the extinction ratio of the transmitted data gradually decreases with increasing injection level, which seriously degrades the noise and the bit-error-rate performance. If the transmitted data stream is further monitored, the intensity noise raised by the beating between incoming laser and local FPLD could occur. This phenomenon could also induce an interfered signal inside the FPLD transmitter. In particular, when the injecting wavelength is slightly deviated from the mode wavelength, the interference occurs to greatly enlarge the relative intensity noise of the transmitted data and thus induces additional chirp for output data stream. This is why the external injection is limited to below +3 dBm. Otherwise, such an interference problem becomes so serious as to degrade the transmitted data performance.

D. Performances of the MCU-Based Auto-Restorable Injection-Locking System

To obtain the BER performance, the DC bias current of the FPLD is set as 30 mA and the amplitude of the pseudo random

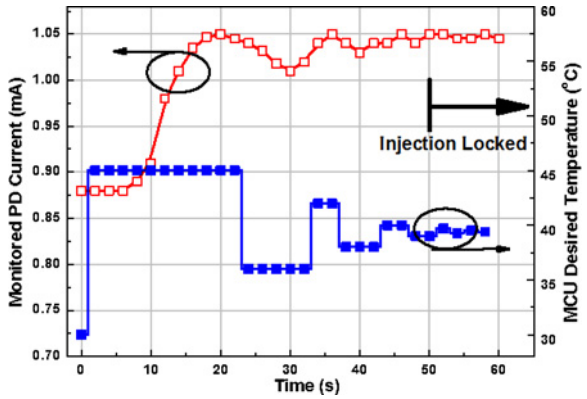

Fig. 8. Recovery experience of the self-restorable unlocked FPLD and corresponding MPD current controlled by MCU.

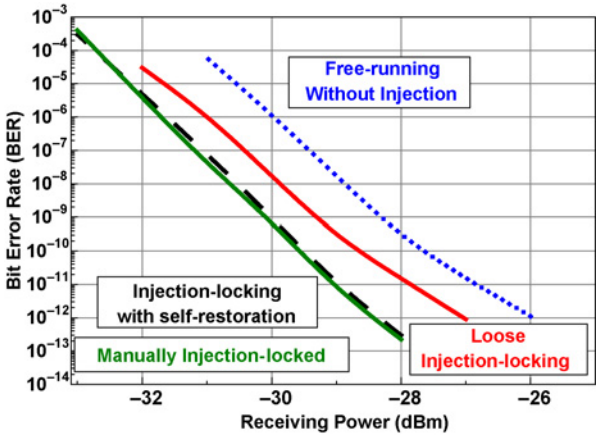

Fig. 9. BER of the FPLD transmitter measured at three different conditions.

binary sequence (PRBS) datastream to directly modulate the FPLD is set to reach an on/off extinction ratio of 10 dB. The FPLD temperature is controlled at 25 °C. In Fig. 9, the BER performance was analyzed at back-to-back condition without the use of any WDM filter between FPLD and receiver, as shown in Fig. 1 of the manuscript. First of all, the BER performances of the FPLD working at free-running and manually operated to reach a perfectly injection-locking condition are measured and shown as the blue and green curves, respectively. Without perfect matching between the FPLD mode and the external injection wavelength (i.e., the loose injection-locking condition), the BER significantly degrades with its response curve located between those of the free-running and manually injection-locking cases. The BER response obtained when detuning the injection wavelength away from the FPLD mode by only 0.03 nm is shown as the red curve in Fig. 9.

Afterward, the MPD-MCU based self-restorable injection-locker is initiated to achieve auto-restoration injection-locking, and the measured BER response (black dashed curve) shows almost identical response with the best case obtained at manually injection-locking condition. Note that the auto-restoration speed strictly depends on the cooling/heating efficiency of the TEC and the environmental temperature. Such a long lock-in time is the worst case only when the TEC chip for controlling the temperature of the FPLD is located outside

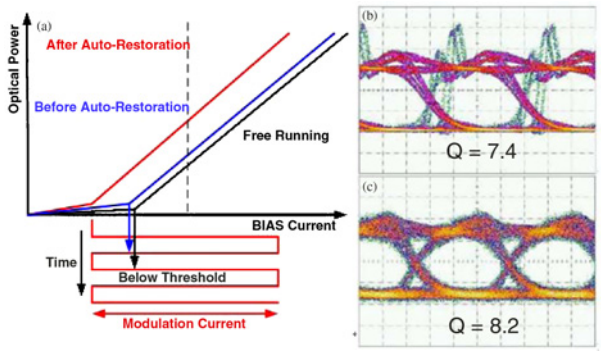

Fig. 10. (a) Threshold current of FPLD before and after self-restoration. Right: The Optical eye-diagrams (b) before and (c) after auto-restoration.

the transmitter module. Therefore, a delayed temperature compensating response is inevitably observed, which can be greatly improved by adding high-power or built-in TEC. A commercially available FPLD TO-can module with a built-in TEC device [12] has been introduced recently in the market, which could greatly shorten the temperature compensation response as well as the lock-in speed through the proposed self-restoration scheme. In addition, the measured BER of the optical transmitting eye diagram can accurately calculate from the recorded Q factor [13]. At 2.5 Gbit/s, the BER of the injection-locked FPLD modulated by PRBS datasteam with $2^{31}-1$ pattern length is 10^{-12} at a receiving power of -25 dBm. After the self-restoration, the Q factor measured from the optical eye histogram is as much as 8.2, providing a reachable BER of 1.1×10^{-16} at a data rate of 2.5 Gbit/s.

The optical eye-diagram and Q value of before and after auto-restoration are shown in Fig. 10. The lower Q value of about 7.4 caused by the significant overshoot of the FPLD transmitted data-stream is obtained before auto-restoration condition, which is mainly attributed to the lower bias point and modulation base below the FPLD threshold current as shown in Fig. 10(a) and (b). After auto-restorable injection-locking operation, the threshold current of FPLD is effectively decreased due to the optical injection at a proper wavelength coincident with the longitudinal mode of the FPLD [5], such that the overshoot problem observed on the eye-diagram is solved and the Q value can be further promoted to 8.2 or larger as shown in Fig. 10(c). We have also measured the BER performances by slightly detuning the wavelength of incoming source away from that of the free-running FPLD at very beginning, then comparing the receiving sensitivity of FPLD before and after self-restoration control, as shown in Fig. 11. Without the self-restoration scheme, the degradation on BER performance of the injected FPLD transmitter becomes serious with increasing wavelength deviation. In comparison, the power penalty for obtaining the same BER at 10^{-9} from the injection-locked FPLD transmitter without a self-restoration control greatly increases from 0.8 to 1.9 dB as the deviated wavelength enlarges from 0.02 to 0.04 nm. After self-restoration control, the mode wavelength of the FPLD eventually coincides with that of the incoming source to results in a receiving sensitivity of -30.1 and -28.2 dBm at BER of 10^{-9} and 10^{-12}, respectively.

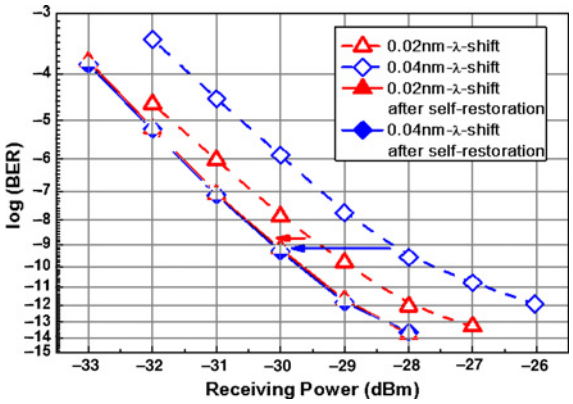

Fig. 11. BER of the FPLD transmitter before and after self-restoration at different wavelength-deviation conditions.

TABLE I
EXPENSE COMPARISON OF THE INJECTION-LOCKED TRANSMITTER SOLUTIONS BETWEEN RSOA AND FPLD WITH/WITHOUT SELF-RESTORATION

System / Expense	RSOA WDM-PON	Injection-Locked FPLD With Self-Restoration	Injection-Locked FPLD Without Self-Restoration
Light source	U.S.$500–1000	U.S.$5–20	U.S.$5–20
TEC controller	U.S.$10	U.S.$10	U.S.$10
MPD-MCU	–	U.S.$ ~1	–

The additional cost is an important issue for the implementation of the self-restorable injection-locked FPLD in practical networks. The component expense of the proposed self-restorable injection-locking FPLD scheme is briefly listed as Table I, which is compared with the reflective semiconductor optical amplifier (RSOA) based injection-locked transmitter [14] and the traditional coherent wavelength injection locked FPLD without self-restorable function. As compared with the RSOA (OA-RL-OEC-1550, CIP) based injection-locked transmitter, a great reduction on the cost at the light source is reached due to the use of a commercially available FPLD in our scheme. The TEC cooler and controller are necessary for all architectures. Only the cost of an ADC/DAC integrated MCU controller is added into the proposed scheme, but the market price of a popular MCU (such as the ATMEL MEGA88V) used in commercial systems is just $1 USD.

For the future integration of optical transceiver in the proposed system, a schematic diagram was modified from a typical 2.5 Gb/s small-form-factor-pluggable (SFP) optical transceiver (SI1525-40ATO, SANOC). Most of the components in the system are commercial and ready-to-use parts in a typical SFP transceiver application. For example, the laser diode driver, limiting amplifier, TEC controller, MCU, and PIN-TIA receiver were chosen as MAX3738 (MAXIM), MAX3747 (MAXIM), MAX8521 (MAXIM), ATMEGA88 (ATMEL), and TRR-1F41-320 (Truelight), respectively. In particular, the proposed system needs to control the temperature of the FPLD and a TEC cooler should be integrated in the transceiver. A commercial laser TO-can module built-in TEC cooler [12] with a maximum diameter of 5.6 mm and a total length of 12.7 mm was demonstrated by Sumitomo Electric Industries, Ltd. as shown in Fig. 12. By implanting such a transmitter, the system could be achieved in a compact-size module such as a typical SFP optical transceiver for future access networks and LAN application.

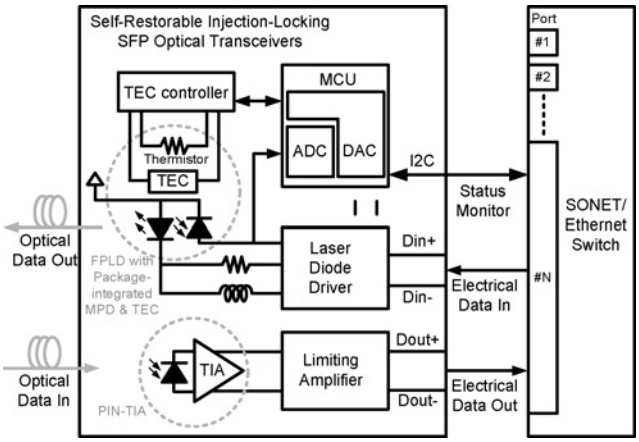

Fig. 12. Future system of the MPD-MCU based self-restoration unit.

IV. CONCLUSION

A novel *in situ* and self-restorable scheme has been demonstrated for the injection-locking FPLD-based WDM transmitter by an integrated MPD in connection with an MCU controlling unit. The injection-locking and self-restoration characteristics such as the locking-in wavelength range and the illuminated power dependent MPD current of the injection-locked FPLD are analyzed. The integrated MCU calculates the monitored photocurrent from the MPD and dynamically controls the FPLD temperature via a TEC controller. After self-restorable injection locking, the transmitter exhibits a Q factor of 8.2 to provide a reachable BER as low as 1.1×10^{-16}, and an SMSR of >35 dB. The FPLD directly modulated by a PRBS datasteam can be self-restoration injection-locked within 50 s, achieving a BER of 10^{-12} at a data rate of 2.5 Gbit/s with a receiving power as low as −25 dBm. With the self-restorable injection-locking scheme, the APC function that was prohibited in the injection-locked FPLDs can be added into future FPLD-based optical networks with a vastly improved stability and reliability. The proposed scheme works for most of the injection-locking FPLDs and can be cost effectively implemented using a minimum amount of redundant network resources.

REFERENCES

[1] C. Henry, N. A. Olsson, and N. K. Dutta, "Locking range and stability of injection locked 1.54 mm InGaAsP semiconductor laser," *IEEE J. Quantum Electron.*, vol. 21, no. 8, pp. 1152–1156, Aug. 1985.

[2] Y. Matsui, S. Kutsuzawa, S. Arahira, Y. Ogawa, and A. Suzuki, "Bifurcation in 20-GHz gain-switched 1.55-μm MQW lasers and its control by CW injection seeding," *IEEE J. Quantum Electron.*, vol. 34, no. 7, pp. 1213–1223, Jul. 1998.

[3] Z. Xu, Y.-J. Wen, W.-D. Zhong, C.-J. Chae, X.-F. Cheng, Y. Wang, C. Lu, and J. Shankar, "High-speed WDM-PON using CW injectionlocked Fabry-Pérot laser diodes," *Opt. Express.*, vol. 15, no. 6, pp. 2953–2962, 2007.

[4] N. Kashima, S. Yamaguchi, and S. Ishii, "Optical transmitter using side-mode injection locking for high-speed photonic LANs," *IEEE J. Lightwave Technology*, vol. 22, no. 2, pp. 550–557, Feb. 2004.
[5] Y.-C. Chang, Y.-H. Lin, J. H. Chen, and G.-R. Lin, "All-optical NRZ-to-PRZ format transformer with an injection-locked Fabry-Perot laser diode at unlasing condition," *Opt. Express*, vol. 12, no. 19, pp. 4449–4456, Sep. 2004.
[6] C. K. Chan, F. Tong, L. K. Chen, K. P. Ho, and D. Lam, "Fiber-fault identification for branched access networks using a wavelength-sweeping monitoring source," *IEEE Photon. Technol. Lett.*, vol. 11, no. 5, pp. 614–616, May 1999.
[7] K. Lee, S. B. Lee, J. H. Lee, Y.-G. Han, S.-G. Mun, S.-M. Lee, and C.-H. Lee, "A self-restorable architecture for bidirectional wavelength-division-multiplexed passive optical network with colorless ONUs," *Opt. Express*, vol. 15, no. 8, pp. 4863–4868, Apr. 2007.
[8] R. D. Esman and L. Goldberg, "Simple measurement of laser diode spectral linewidth using modulation sidebands," *Electron. Lett.*, vol. 24, no. 22, pp. 1393–1395, Oct. 1988.
[9] S. Bouchoule, N. Stelmakh, M. Cavelier, and J.-M. Lourtioz, "Highly attenuating external cavity for picosecond-tunable pulse generation from gain/Q-switched laser diodes," *IEEE J. Quantum Electron.*, vol. 29, no. 6, pp. 1693–1700, Jun. 1993.
[10] L. Li, "Static and dynamic properties of injection-locked semiconductor lasers," *IEEE J. Quantum Electron.*, vol. 30, no. 8, pp. 1701–1708, Aug. 1994.
[11] K. Petermann, *Laser Diode Modulation and Noise*. Dordrecht, The Netherlands: Kluwer Academic, 1998.
[12] M. Ichino, S. Yoshikawa, H. Oomori, Y. Maeda, N. Nishiyama, T. Takayama, T. Mizue, I. Tounai, and M. Nishie, "Small form factor pluggable optical transceiver module with extremely low power consumption for dense wavelength division multiplexing applications," in *Proc. Electron. Compon. Technol. Conf.*, vol. 1. 2005, pp. 1044–1049.
[13] N. S. Bergano, F. W. Kerfoot, and C. R. Davidsion, "Margin measurements in optical amplifier system," *IEEE Photon. Technol. Lett.*, vol. 5, no. 3, pp. 304–306, Mar. 1993.
[14] W. Lee, M.-Y. Park, S.-H. Cho, J. Lee, C. Kim, G. Jeong, and B.-W. Kim, "Bidirectional WDM-PON based on gain-saturated reflective semiconductor optical amplifiers," *IEEE Photon. Technol. Lett.*, vol. 17, no. 11, pp. 2460–2462, Nov. 2005.

Gong-Ru Lin (S'93–M'96–SM'04) received the B.S. degree in physics from Soochow University, Taipei, Taiwan, in 1990, and the M.S. and Ph.D. degrees in electro-optical engineering from National Chiao Tung University, Hsinchu, Taiwan, in 1990 and 1996, respectively.

He was a Faculty Member of several universities from 1997 to 2006. He joined the Graduate Institute of Photonics and Optoelectronics (GIPO) and the Department of Electrical Engineering, National Taiwan University (NT), Taipei, Taiwan as a Full Professor in 2006. He is currently directing the Laboratory of Fiber Laser Communications and Si Nano-Photonics. His current research interests include fiber-optic communications, all-optical data processing, femtosecond fiber lasers, nanocrystallite Si photonics, ultrafast photoconductors, and optoelectronic phase-locked loops.

Dr. Lin is a member of the Optical Society of America, a Fellow of the International Society for Optical Engineers (FSPIE), a Fellow of the Institution of Engineering and Technology (FIET), and a Fellow of British Institute of Optics (FInstP). He is currently the Deputy Chair with GIPO, NT, and the Chair of IEEE Lasers and Electro-Optics Society, Taipei Chapter.

Yu-Sheng Liao received the B.S. degree in applied mathematics and electrical engineering from the National Chiao Tung University (NCTU), Hsinchu, Taiwan, in 2002. He is currently pursuing the Ph.D. degree from the Department of Photonics and Institute of Electro-Optical Engineering, NCTU.

He has co-authored more than ten papers in international periodicals and over 20 papers in international conferences. His current research interests include fiber-optic communications, all-optical data processing, and millimeter-wave photonic phase-locked loops.

Hao-Chung Kuo received the B.S. degree in physics from National Taiwan University, Taipei, Taiwan, in 1990, and the M.S. degree in electrical and computer engineering from Rutgers University, New Brunswick, NJ, in 1995, and the Ph.D. degree in electrical and computer engineering from the University of Illinois at Urbana-Champaign, Champaign, in 1999.

He has an extensive professional career, both in research and industrial research institutions. He was a Research Consultant with Lucent Technologies, Bell Labs, Murray Hill, NJ, from 1995 to 1997, a Research and Development Engineer with the Fiber-Optics Division, Agilent Technologies, Santa Clara, CA, from 1999 to 2001, and a Research and Development Manager with LuxNet Corporation, Fremont, CA, from 2001 to 2002. In 2002, he joined National Chiao Tung University, Hsinchu, Taiwan as a Faculty Member with the Institute of Electro-Optical Engineering. He has authored or co-authored over 60 publications. His current research interests include the epitaxy, design, fabrication, and measurement of high-speed InP and GaAs-based vertical-cavity surface-emitting lasers, as well as GaN-based light-emitting devices and nanostructures.